Journal of Water Science and Engineering

Research Article

Large Specific Surface Area Nitrogen-Doped Biochar Cathode: A Tactics for Recycling Nitrogen and Phosphorus Enriched Aquatic Plant

Chen L, Zhou L and Sun J*

Key Laboratory of Catalysis and Materials Science of the State Ethnic Affairs Commission & Ministry of Education, Hubei Province, College of Resource and Environmental Science, South-Central University for Nationalities, Wuhan 430074, PR China

Volume 1 Issue 4 - 2019
Received Date: 02 July 2019
Accepted Date: 19 July 2019
Published Date: 23 July 2019

1. Abstract

In this study, a nitrogen-doped biochar oxygen reduction reaction(ORR) cathode(Alternanthera philoxeroidescarbon) was produced by two kinds of molten salts ($ZnCl_2$ and $Mg_5(OH)_2(CO_3)_4$) carbonization without extra nitrogen source, which had an excellent performance in Electro-Fenton (E-Fenton) process. The result of BET shows that the biochar carbon had a large specific surface area (1154.179 $cm^2 \cdot g^{-1}$). Moreover, the XPS and SEM results show that both pyridinic-N and graphitic-N existed in the biochar carbon and it had a Honeycomb structure surface, which has a positive effect on the production of H_2O_2(producing yield 0.9 $mmol \cdot L^{-1}$).Further, degradation efficiency of X3B in 20min was more than 90% and the reaction kinetic constant was 0.153min^{-1}.

2. Keywords

Nitrogen and phosphorus enriched; Aquatic plant; Biochar; E-Fenton; ORR; Molten salt

3. Introduction

E-Fenton technology is a kind of advance oxidation process-derived from traditional Fenton technology, which has been reported as a high-efficiency combined technology in contaminants degradation [1]. H_2O_2 was in situ produced by O_2 through cathodic $2e^-$ ORR under the catalysis of Fe^{2+}, generating hydroxyl radical (•OH) with very strong oxidizing power. This in situ generation of H_2O_2 can avoid the risks of its storage and transport, played a very important role in E-Fenton effect. Therefore, enhancing the efficiency of $2e^-$ ORR is a kind of the pivotal method in the study of E-Fenton technology [2-3].

For the past few years,carbon materials were widely used in E-Fenton technology to improve the Hydrogen peroxide production because of their high potential for hydrogen evolution, low catalytic activity in H_2O_2 decomposition, good conductivity and stability [4]. At present,a large bunch of N-doped carbon materials arise and exhibit high electrocatalytic activity [5].Nitrogen species has been proved to be active sites for ORR. But the function of different kinds of N in ORR is still discussed.Generally speaking,the graphitic-N improves the electron transfer efficiency of carbon materials. At the same time, the ORR current density is affected by the total content of graphitic and pyridinic-N [6-7]. Nevertheless, because of the extrinsic various precursors, such as extra nitrogen sources and organic template, the preparation of these materials is complicated and high costs [8]. Step by step, biochar has become a priority choice in cathode material precursor because of its large specific surface area, which provides sufficient reaction space.

A nitrogen and phosphorus enriched aquatic plant named Alternanthera philoxeroides (Latin Name: Alternanthera philoxeroides (Mart.) Griseb.) which was imported into China in 20th century from Brazil for the solution of feed shortage. But phenomenon of eutrophication supplies plenty nutrition for the growth of Alternanthera philoxeroides which directly cause river blocking and polluting. Due to the high survival rate, it is difficult to clear up these plants on the river. Differed from other Biomass materials, Alternanthera philoxeroides is an invasive alien species, grown fast and cheap. It is worth mentioning that Alternanthera philoxeroides can enrich nitrogen and phosphorus from the eutrophic water. We make an assumption that after a high temperature handle, these original nitrogen species in the plants can be used to

***Corresponding Author (s):** Jie Sun, Key Laboratory of Catalysis and Materials Science of the State Ethnic Affairs Commission & Ministry of Education, Hubei Province, College of Resource and Environmental Science, South-Central University for Nationalities, Wuhan 430074, PR China, Tel:+86 13476035879; E-mail:jetsun@mail.scuec.edu.cn*

Citation: Sun J, Large Specific Surface Area Nitrogen-Doped Biochar Cathode: A Tactics for Recycling Nitrogen and Phosphorus Enriched Aquatic Plant. Journal of Water Science and Engineering. 2019; 1(4): 1-5.

produce ORR electrocatalytic active sites on the surface of cathode. Thus, Alternanthera philoxeroides biochar was equipped as a cathode material applied in E-Fenton technology. Not only that, molten salt $ZnCl_2$ and $Mg_5(OH)_2(CO_3)_4$ is prepared for further unearthing the electrocatalytic potential of the biochar.

4. Material and Methods

4.1. The production and the activation of alternanthera philoxeroides carbon

Firstly, the Alternanthera philoxeroides were washed by distilled water and reserved the stem to product biochar. Next the stem dried in draught drying cabinet in 378 K for 48 h, and it was smashed by ball grinding mill. After dehydration, each 2.0g of Alternanthera philoxeroides powder was mixed up with the rate of $ZnCl_2$ (AR) and $Mg_5(OH)_2(CO_3)_4$ (AR) from 1:3:1, 1:0:0, 1:0:1 to 1:3:0, which respectively corresponding from sample C_{131}, C_{100}, C_{101} to C_{130}. Carbonization was performed in a tube furnace under a N_2 gas flow at 973 K for 2 h. The carbonization samples were dipped in 2 mol· L^{-1} HCl (AR) for 12 h and then washed by deionized water.Finally, the products were dried at 333 K in an oven.

4.2. Fabrication of biochar electrode

80 wt.% Alternanthera philoxeroides biochar powder, 10 wt.% acetylene black and 10 wt.% PTFE were mixed to produce Electrodes. The mixture was stirred with ethyl alcohol for 12 h to ensure homogeneity and then pressed onto titanium mesh.

4.3. Material characterization

X-ray Photoelectron Spectroscopy (XPS) measurements (on a MULTILAB2000* X-ray photoelectron spectrometer) were used to evaluate the elements on the surface of biochar samples. Surface morphology of biochar samples were observed by field emission scanning electron microscopy (SEM) in 1.5 KV deceleration voltage.Brunauer-Emmett-Teller (BET) measurements (JWGB SCI.& TECH, JW-BK132F, China) determined N_2 adsorption/desorption.

An electrochemical workstation (CHI-660E, China) was used to analyze electrochemical impedance spectroscopy (EIS) measurements. The initial potential was set as open circuit potential and the range of angular frequency was applied from 0.01 Hz to 100 k Hz.Butler-Volmer equation (Eq.1) was adopted to calculate Cathode oxygen diffusion coefficient.

$$D_2 = \frac{R^2T^2}{2A_1^2n_1^4F^4c^2\sigma^2} \qquad (1)$$

Where D_2 is oxygen diffusion coefficient ($cm^2 \cdot s^{-1}$) and R is the perfect gas constant (8.314 $J \cdot mol^{-1} \cdot K^{-1}$), T is the reaction temperature (K), A_1 is the Macroscopic area of material(cm^2), n_1 is the number of reaction electron transfer, F is the Faraday coefficient (96,500 $C \cdot mol^{-1}$), c is the Oxygen concentration in the solid phase($mol \cdot cm^{-3}$) and σ is Warburg coefficient.

4.4. E-Fenton degradation process

the E-Fenton degradation process was carried out in an 80 mL beaker containing 50 mL of simulated wastewater (50 $mg \cdot L^{-1}$ X3B,0.1 $mol \cdot L^{-1}$ Na_2SO_4,0.1$mmol \cdot L^{-1}$ Fe^{2+}, PH=3) and equipped with three electrodes at room temperature. The concentration of X3B was measurand by ultraviolet-visible spectrophotometer (Shimadzu Co., UV2450, Japan) at 530nm wavelength.

4.5. H_2O_2 producing detection and trapping of the Yydroxyl radical

The concentration of H_2O_2 formed during the E-Fenton process was detected by the potassium titanium (IV) oxalate method [9-10]. The treated water samples 0.5 mL and titanium reagent 0.5mL were added into 1.5 mL deionized water. Measure the absorbance of the mixture by ultraviolet-visible spectrophotometer at 400 nm wavelength. The current efficiency of H_2O_2 production was

calculated by Faraday (Eq.2) [10-11].

$$CE = \frac{nFC_{H_2O_2}V}{\int_0^t Idt} \times 100\% \qquad (2)$$

The hydroxyl radical concentration was analyzed by chemical fluorometric enzyme immunoassay method through coumarin trapping. Instantly, the reaction between non-fluorescent coumarin and hydroxyl radical produces highly fluorescent 7-hydroxycoumarin which has a Strong fluorescence absorption at 450 nm.

5. Result and Discussion

5.1. Surface elemental analysis

According to **Figure 1**, The surface XPS full spectrum of C_{100}, C_{101}, C_{130} and C_{131} was showed the element species and the proportion of active carbon surface elements in Alternanthera philoxeroides was shown in **Table 1**. The percentage of elements relative to the atom can be derived [10-12]. Binding energies of around 284.6, 401.0, 532.6, 1022.0 and 1045.0 eV may be assigned to C 1 s, N 1 s, O 1 s, Zn $2p_{3/2}$, and Zn $2p_{1/2}$, respectively [13]. Mg was not detected inthose samples. Little Zn was detected on C_{130} (0.33%) and C_{131} (0.32%) which mean Zn have been solved in the reaction. All those samples have nitrogen and the N-component peaks were shown in **Figure 2**.

Both graphitic-N and pyridinic-N exist in the sample [14-15]. Pyridinic-N species dominate the ORR electro catalytic active sites under acidic conditions and graphitic-N dedicate for electrons transfer efficiency [16-17]. All in all, a high ORR electrochemistry activity of cathode material can only be achieved by the existence of both nitrogen species.

Table 1: proportion of active carbon surface elements in alternanthera philoxeroides.

sample	Element Species			
	C	O	N	Zn
C_{100}	89.14%	8.94%	1.93%	-
C_{101}	85.90%	11.78%	2.32%	-
C_{130}	92.81%	5.08%	1.78%	0.33%
C_{131}	93.58%	4.64%	1.47%	0.32%

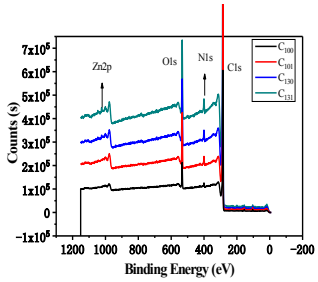

Figure 1: The surface XPS full spectrum of C100, C101, C130 and C131.

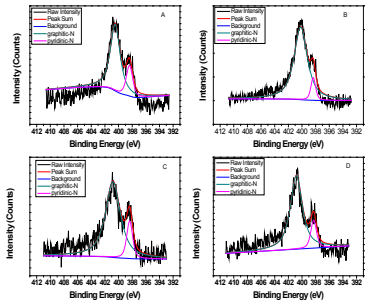

Figure 2: N-component peaks for (A) C100 (B) C101 (C) C130 (D) C131.

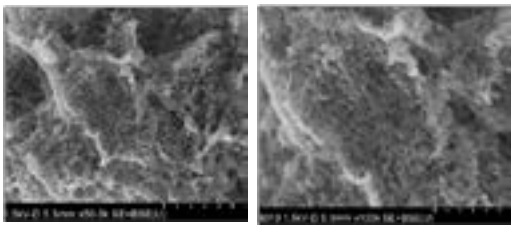

Figure 3: SEM of C131.

5.2. Morphology and channel structure analysis

The surface of the sample was observed by field emission scanning electron microscopy (SEM).

N_2 adsorption/desorption was measured by BET measurements. Normally, Adsorption and desorption curves of nitrogen was measured firstly, and then, through calculating, got the Specific surface area and aperture distribution. The Isothermal adsorption desorption curve of C_{100}, C_{101}, C_{130} and C_{131} was measured in Figure 4 & 4 and the Pore size distribution of them was measured in **Figure 5**. Data was processed in the **Table 2**. The specific surface area of C_{100}, C_{101}, C_{130}, C_{131} was 1099.113 ($cm^2 \cdot g^{-1}$), 991.950($cm^2 \cdot g_{-1}$), 1306.478($cm^2 \cdot g^{-1}$), 1154.179($cm^2 \cdot g^{-1}$), respectively. The total pore volume of them was 1.1439 ($cm^3 \cdot g^{-1}$), 1.0414 ($cm^3 \cdot g^{-1}$), 1.7295 ($cm^3 \cdot g^{-1}$), 1.5950 ($cm^3 \cdot g^{-1}$), and the average pore size of them was 2.294 (nm), 2.466(nm), 3.751(nm), 3.888(nm). As the rising of temperature, $ZnCl_2$ was transformed to ZnO. When the temperature rises above 600℃, Carbon starts to form, ZnO was further reduced to single substance. Mesoporous and microporous were produced in the carbon skeleton because of the in situ generated Zn can sublimate. The larger specific surface area it has, the more activity reactive site it provides and the $2e^-$ ORR reaction started drastically. It made the in situ generated H_2O_2 full contact with iron in solution and accelerate degradation of organic pollutants.

5.3. Electrochemical analysis

The charge transfer resistance (R_c) from C_{100} to C_{131} was analyzed by the Nyquist plot. The results were shown in **Figure 6**. High frequency semicircle in accordance with the charge transfer resistance dominant kinetics at the electrode interface while the low frequency straight sloping line correlated to the diffusion process between the electrode and the electrolyte [18]. According to **Figure 7**, The order of Warburg constants from large to small is C_{101}(0.2752), C131(0.2652), C_{100}(0.2183), C_{130}(0.1632). So the order of diffusion coefficient from large to small is C_{130}, C_{100} , C_{131}, C_{101}. The diffusion coefficient is related to the specific surface area of the material. The bigger bore diameter it had, the Better oxygen diffusion efficiency it had.

5.4. X3B degradation

As an azo dye, X3B contains an azo bond, which is the key group that's colored X3B. In **Figure 8**, X3B was rapidly degraded by all of the samples with removal efficiency of more than 90% in 15 min. What's more, the degradation fitting of X3B obey pseudo-first-order reaction rate kinetics. Thekinetic constant form C_{100} to C_{131} was 0.1787 (min^{-1}), 0.1688 (min^{-1}), 0.1810 (min^{-1}), 0.1533 (min^{-1}), severally.

5.4. H_2O_2 producing yield and trapping of the hydroxyl radical

In E-Fenton system, the yield of H_2O_2 is a very important indica-

Table 2: specific surface area, total pore volume and average pore size of different cathode carbon materials.

sample name	S_{BET} ($cm^2 \cdot g^{-1}$)	volume ($cm^3 \cdot g^{-1}$)	average pore size(nm)
C_{100}	1099.113	1.1439	2.294
C_{101}	991.950	1.0414	2.466
C_{130}	1306.478	1.7295	3.751
$_{C1}31$	1154.179	1.5950	3.888

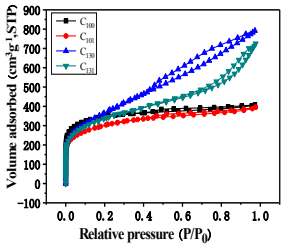

Figure 4: Isothermal adsorption desorption curve of C100, C101, C130 and C131.

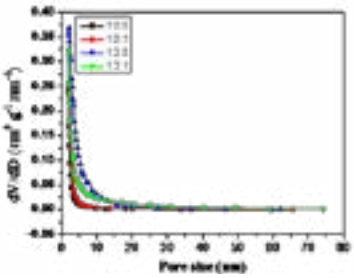

Figure 5: Pore size distribution of C100, C101, C130 and C131.

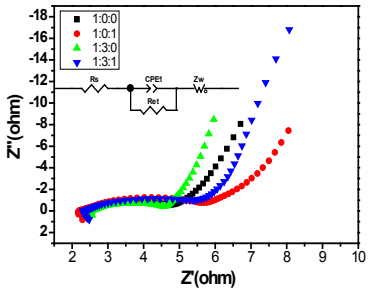

Figure 6: Nyquist plot of C100, C101, C130 and C131.

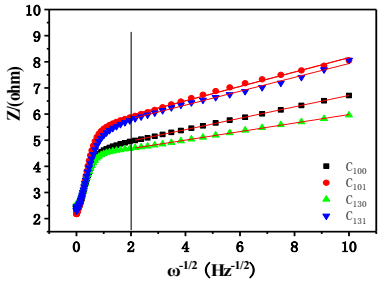

Figure 7: Warburg impedance of C100, C101, C130 and C131.

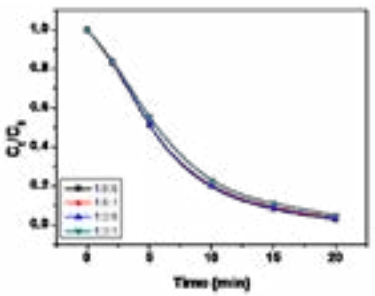

Figure 8: X3B Degradation by C100, C101, C130 and C131 and corresponding kinetic constant.

tor [19]. So, it was measured in the same potential. in **Figure 9** and **Figure 10**, the maximum product (0.9 mM) and current efficiency (40%) of H_2O_2 was observed in C_{131}, it means the C_{131} had the best electro-catalytic property.

hydroxyl radical is a kind of product of Fenton reaction, has non-selective strong oxidation capacity,can mine organic pollutants into H_2O and CO_2.

In **Figure 11**, fluorescence intensity change diagram of C_{131} at different reaction time illustrated the yield of hydroxyl radical enhancing through the electro catalysis of C_{131}.

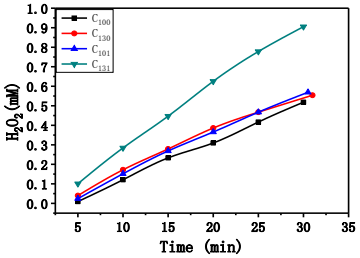

Figure 9: The production of H2O2 at C100, C101, C130 and C131.

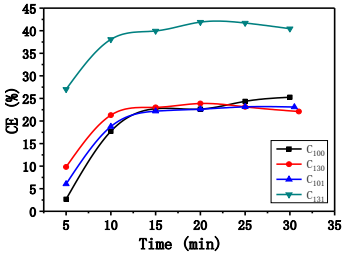

Figure 10: The current efficiency of H2O2 generated at C100, C101, C130 and C131.

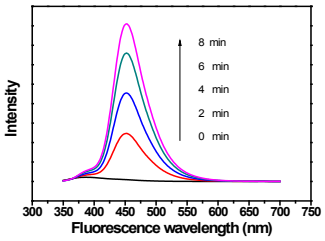

Figure 11: Fluorescence intensity change diagram of C131 at different reaction time.

References

1. Sires I, Brillas E, Oturan MA, Rodrigo MA, Panizza M. Electrochemicaladvanced oxidation processes: today and tomorrow. A review. Environ. Sci. Pollut.Res Int. 2014; 21 (14): 8336-8367.

2. Gao Y, Ji Y, Li G, An T. Theoretical investigation on the kinetics and mechanisms of hydroxyl radical-induced transformation of parabens and its consequences for toxicity: influence of alkyl-chain length. Water Res. 2016; 91: 77-85.

3. Yang H, Zhou M, Yang W, Ren G, Ma L. Rolling-made gas diffusion electrodewith carbon nanotube for electro-Fenton degradation of ace-

tylsalicylic acid. Chemosphere. 2018; 206: 439-446.

4. Gao G, Zhang Q, Hao Z, Vecitis CD. Carbon nanotube membrane stack forflow-through sequential regenerative electro-Fenton. Environ. Sci Technol. 2015; 49 (4): 2375-2383.

5. Yan P, Liu J, Yuan S, Liu Y, Cen W, Chen Y. The promotion effects ofgraphitic and pyridinic N combinational doping on graphene for ORR. ApplSurfSci. 2018; 445: 398-403.

6. Ding W, Wei Z, Chen S, Qi X, Yang T, Hu J, et al. Space-confinement-induced synthesis of pyridinic- and pyrrolic-nitrogendoped graphene for the catalysis of oxygen reduction. Angew. Chem. Int. Ed. Engl. 2013; 52(45): 11755-11759.

7. Zhang C, Hao R, Liao H, Hou Y. Synthesis of amino-functionalized graphene asmetal-free catalyst and exploration of the roles of various nitrogen states in oxygenreduction reaction. Nano Energy. 2013; 2 (1): 88-97.

8. Liu XJ, Zhou YC, Zhou WJ, Li LG, Huang SB, Chen SW.Biomass-derived nitrogen self-doped porous carbon as effective metal-free catalysts for oxygenreduction reaction. Nanoscale. 2015; 7 (14): 6136-6142.

9. Ren W, Tang D, Lu X, Sun J, Li M, Qiu S, Fan D. Novel multilayer ACF@rGO@OMC cathode composite with enhanced activity for electro-fenton degradationof phthalic acid esters. Ind Eng Chem Res. 2016; 55 (42): 11085-11096.

10. Jiaxiang L, Diyong T, Li H, Yifei C, Wei R, Jie S. Oxygen reduction reaction performance nitrogen-doped biochar cathode: A strategy for comprehensive utilizing nitrogen and carbon in water hyacinth. Bioresour. Technol. 2018; 267: 524-531.

11. Zhou M, Yu Q, Lei L. The preparation and characterization of a graphite–PTFEcathode system for the decolorization of C.I. Acid Red 2. Dyes Pigm. 2008; 77 (1): 129-136.

12. Foelske-Schmitz A, Weingarth D, Kötz R. XPS analysis of activated carbonsupported ionic liquids: enhanced purity and reduced charging. Surf. Sci. 2011; 605(23–24): 1979-1985.

13. Madhu R, Veeramani V, Chen SM, Veerakumar P, Liu SB, Miyamoto N. Functional porous carbon-ZnO nanocomposites for high-performance biosensors andenergy storage applications. PCCP. 2016; 18 (24): 16466-16475.

14. Xiao J, Bian X, Liao L, Zhang S, Ji C, Liu B. Nitrogen-doped mesoporousgraphene as a synergistic electrocatalyst matrix for high-performance oxygen reduction reaction. ACS Appl. Mater. Interfaces. 2014; 6 (20): 17654-17660.

15. Yu H, Shang L, Bian T, Shi R, Waterhouse GI, Zhao Y, et al.Nitrogen-doped porous carbon nanosheets templated from gC3 N4 as metal-free electrocatalysts for efficient oxygen reduction reaction. Adv. Mater. 2016; 28 (25): 5080-5086.

16. Cui X, Yang S, Yan X, Leng J, Shuang S, Ajayan PM, et al. Pyridinic-nitrogen-dominated graphene aerogels with Fe-N-C coordination for highly efficientoxygen reduction reaction. Adv. Funct Mater. 2016; 26 (31): 5708-5717.

17. Zhang C, Hao R, Liao H, Hou Y. Synthesis of amino-functionalized graphene asmetal-free catalyst and exploration of the roles of various nitrogen states in oxygenreduction reaction. Nano Energy. 2013; 2 (1): 88-97.

18. Du Y, Feng YJ, Qu YP, Liu J, Ren NQ, LiuH. Electricity generation andpollutant degradation using a novel biocathode coupled photoelectrochemical cell.Environ. Sci. Technol. 2014; 48 (13): 7634-7641.

19. Liu Y, Chen S, Quan X, Yu H, Zhao H, Zhang Y. Efficient mineralization ofperfluorooctanoate by electro-fenton with H2O2 electrogenerated on hierarchicallyporous carbon. Environ. Sci. Technol. 2015; 49 (22): 13528-13533.